Comparison of Contrast-Enhanced Ultrasonograpy with Gd-EOB-DTPA-enhanced MRI in the Diagnosis of Liver Metastasis from Colorectal Cancer

Kazue Shiozawa, MD, PhD,[1] Manabu Watanabe, MD, PhD,[1] Takashi Ikehara, MD, PhD,[1] Yasushi Matsukiyo, MD,[1] Michio Kogame, MD,[1] Yoshinori Kikuchi, MD, PhD,[1] Yuichiro Otsuka, MD, PhD,[2] Hironori Kaneko, MD, PhD,[2] Yoshinori Igarashi, MD, PhD,[1] Yasukiyo Sumino, MD, PhD[1]

[1] Division of Gastroenterology and Hepatology, Department of Internal Medicine,
Toho University Medical Center, Omori Hospital, 6-11-1, Omorinishi, Ota-ku, Tokyo 143-8541, Japan
[2] Department of Surgery, Toho University Medical Center, Omori Hospital, 6-11-1, Omorinishi,
Ota-ku, Tokyo 143-8541, Japan

ABSTRACT: *Purpose.* To compare contrast-enhanced ultrasonography (CEUS) using Sonazoid with Gd-EOB-DTPA-enhanced MRI (EOB-MRI) in the diagnosis of liver metastases in patients with colorectal cancer.

Methods. A total of 69 patients diagnosed with or suspected of having liver metastasis were enrolled. These hepatic lesions were diagnosed by histopathological examination after surgical resection or based on follow-up using various imaging modalities. The diagnostic accuracies of CEUS and EOB-MRI were compared.

Results. One hundred thirty-three lesions were detected. Of these lesions, 109 were diagnosed as liver metastases. Of the 133 lesions, 90.2% were detected on CEUS, and 98.5% on EOB-MRI. One hundred nine lesions were diagnosed as liver metastasis. The areas under the receiver operating characteristic curve for diagnosis were 0.906 and 0.851 on CEUS and EOB-MRI, respectively ($p = 0.41$). Sensitivity, specificity, positive predictive value (PPV), negative predictive value, and overall accuracy were 90.8%, 84.5%, 97.1%, 67.1%, and 90.2%, respectively, for CEUS, and 95.4%, 70.8%, 93.7%, 77.3%, and 91%, respectively, for EOB-MRI.

Conclusions. CEUS has a higher specificity and PPV for the diagnosis of liver metastasis than EOB-MRI. © 2016 The Authors Journal of Clinical Ultrasound Published by Wiley Periodicals, Inc. *J Clin Ultrasound* **45**:138–144, 2017; Published online in Wiley Online Library (wileyonlinelibrary.com). DOI: 10.1002/jcu.22421

Keywords: contrast-enhanced ultrasonography; Gd-EOB-DTPA-enhanced MRI; liver metastasis; colorectal cancer

Correspondence to: M. Watanabe

INTRODUCTION

The liver is the most common site of distant metastasis from colorectal cancer.[1] The standard curative treatment for colorectal liver metastasis in colorectal cancer patients is surgical resection or local treatment with radiofrequency ablation.[2,3] On the other hand, adjuvant therapy, including chemotherapeutic regimens, can induce a favorable response and a longer survival period in patients with unresectable liver metastases by decreasing the tumor extent and rendering the tumor resectable.[4] However,

if chemotherapy is effective, micrometastases may be undetectable by imaging and may be incorrectly judged to have disappeared. To prevent such misjudgment, it is important to detect residual micrometastases after successful chemotherapy before surgical resection.

Recently, the emergence of contrast-enhanced ultrasonography (CEUS) with Sonazoid (Daiichi-Sankyo, Tokyo, Japan) and enhanced MRI with gadolinium-ethoxybenzyl-diethylenetriamine pentaacetic acid (Gd-EOB-DTPA) (Primovist; Bayer Healthcare, Berlin, Germany)—known as EOB-MRI—has improved the detection and diagnosis of malignant liver tumors. Detection of hepatocellular carcinoma (HCC) and liver metastases using CEUS with Sonazoid, dynamic CT, super paramagnetic iron oxide (SPIO)–MRI, and EOB-MRI has been compared,[5–10] but a prospective comparison of the detection of liver metastasis in colorectal cancer using only CEUS with Sonazoid and EOB-MRI has not been reported. In this study, we performed this comparison and investigated the utility of CEUS for diagnosis of liver metastasis of colorectal cancer.

MATERIALS AND METHODS

Sixty-nine patients were diagnosed with colorectal cancer at our hospital between January 2011 and October 2014 and were suspected of having a malignant lesion in the liver on routine gray-scale ultrasonography (US) or dynamic CT and underwent CEUS with Sonazoid and EOB-MRI. These patients included 46 males and 23 females and had a mean age of 66 years (range, 34–86). The primary lesion was located in the rectum in 27 cases, sigmoid colon in 22, transverse colon in 10, ascending colon in 8, and cecum in 2. Patients with five or more masses in the liver were excluded. CEUS and EOB-MRI were performed within 1 month of each other.

All CEUS was performed by two sonographers using an Aplio XG (Toshiba Medical Systems, Tokyo, Japan) with a convex probe (PVT-375BT, 3.75-MHz center frequency). The mechanical index (MI) for the acoustic output was set to 0.2. In patients in whom lesions were detected by gray-scale US, the single focus point was set at the lower margin of the lesion. An intravenous bolus injection of Sonazoid (0.5 ml) was administered via a left cubital venous line followed by flushing with 10 ml of normal saline. The dynamics of enhancement of the lesion were observed in the vascular phase (arterial phase [0–40 seconds], portal venous phase [40–

120 seconds], late phase [>120 seconds]), and in all patients, including those with no lesion visualized on gray-scale US, the whole liver was observed in the postvascular phase 10 minutes after injection, and the presence of defects was evaluated. Visualized defects were examined using defect reperfusion imaging,[11] in which Sonazoid (0.5 ml) was reinjected intravenously and the enhancement dynamics were observed to diagnose metastatic liver cancer. Video images in the vascular and postvascular phases were recorded and analyzed by an off-line procedure. Diagnostic criteria for liver metastases were early washout, usually in the portal venous phase, and hypoenhancement during the portal venous and late phases.[12] EOB-MRI was performed with a 1.5-T superconducting magnet (Signa Lx; GE Healthcare, Milwaukee, WI) and an 8-channel phased-array coil. Fast spoiled gradient-echo T1-weighted images (T1WI), respiratory-triggered fat-saturated fast spin-echo T2-weighted images (T2WI), and single-shot spin-echo echo-planar diffusion-weighted images (DWI) were obtained before contrast administration. Dynamic fat-suppressed gradient-echo T1WI with a three-dimensional acquisition sequence (liver acquisition with volume acceleration) were obtained before (precontrast) and at 20 and 60 seconds and 2, 5, 10, and 20 minutes after administration of EOB. The contrast material (0.025 mmol/kg of body weight) was then administered intravenously via a cubital line, which was flushed with 20 ml of saline using a power injector. Images were acquired in the transverse plane. Images in the sagittal plane were also obtained for the hepatobiliary phase (HBP) 20 minutes after injection of the contrast agent. On EOB-MRI, a lesion was considered a metastasis if it had an intermediately intense signal on T2-weighted images, a hypointense signal on T1WI, high signal intensity on diffusion-weighted images, a faint peripheral ringlike enhancement on the arterial and portal phases, and a hypointense signal on the HBP.[13]

The final diagnosis of liver metastasis was made by histopathological examination of surgically resected specimens or based on course observation (changes of size, such as tumor enlargement and shrinkage) using various imaging modalities. The presence (number of tumors) and qualitative diagnoses of the finally diagnosed metastatic lesions were prospectively compared between CEUS and EOB-MRI. All CEUS and EOB-MRI images were reviewed by a hepatologist with 30 years of experience and a radiologist with 15 years of experience. For

TABLE 1
**Of All 69 Patients with 133 Liver Tumors, Patients' Charac-
teristics, Locations of Primary Lesions and Liver Tumors,
Size of Liver Tumors, Diagnosis of Liver Tumors, Methods of
Final Diagnosis of Liver Tumors, and Interval Between Per-
formances of Contrast-Enhanced Ultrasonography (CEUS)
and Gd-EOB-DTPA-enhanced MRI (EOB-MRI)**

Characteristics	All (n = 69)
Age (years) (mean ± SD)	66 ± 12
Gender	
Male/female	46/23
Locations of primary lesions	
Rectum	27
Sigmoid colon	22
Descending colon	0
Transverse colon	10
Ascending colon	8
Cecum	2
Liver tumors	133
Liver metastases/others	109/24
Others	
Hepatic hemangioma	11
Liver cyst	9
Hepatocellular carcinoma	2
Bile duct adenoma	1
Necrosis after treatment	1
Tumor size (mm) (mean ± SD)	21.3 ± 17.9
Locations of liver tumors	
(Couinaud's segment)	
S1	2
S2	7
S3	11
S4	23
S5	14
S6	25
S7	20
S8	31
Final definite diagnosis	
Histopathological examination	61
Various imaging modalities	72
Interval between performance of	11 ± 12.5
CEUS and EOB-MRI (days) (mean ± SD)	

Abbreviations: CEUS, contrast-enhanced ultrasonography; EOB-MRI: Gd-EOB-DTPA enhanced-MRI.

qualitative diagnosis, tumors were evaluated using the following five-point confidence scale: 1 = definitely not metastasis or absence; 2 = probably not metastasis; 3 = indeterminate; 4 = probably metastasis; 5 = definitely metastasis. Both imaging diagnoses were subjected to receiver operating characteristic (ROC) curve analysis, and the area under the ROC curve (AUC) was calculated. The ROC curves were analyzed using a two-tailed Student's t test for paired data. Based on a score of 4 or 5 on the confidence scale indicating liver metastasis, the sensitivity, specificity, positive predictive value (PPV), negative predictive value (NPV), and accuracy of the diagnosis were calculated and compared between CEUS and EOB-MRI, with $p < 0.05$ regarded as significant. Findings on CEUS and EOB-MRI were judged independently by sonographers and radiologists,

respectively. The study was performed after approval by the Ethics Committee of Toho University Medical Center Omori Hospital.

RESULTS

There were 133 lesions found in the 69 patients, giving a mean number of 1.9 lesions per patient. The mean tumor diameter of all 133 lesions was 21 ± 18 mm. Of these lesions, 109 were diagnosed as metastases and 24 as nonmetastasis, with 61 diagnosed histopathologically and 72 diagnosed based on follow-up of at least 6 months using various imaging modalities. The 24 lesions diagnosed as nonmetastasis were 11 hemangiomas, 9 cysts, 2 HCCs (Figure 1), 1 bile duct adenoma, and 1 focus of necrosis after treatment. Regarding the location, 2, 7, 11, 23, 14, 25, 20, and 31 lesions were present in the segments S1, S2, S3, S4, S5, S6, S7, and S8, respectively. The mean interval between performance of CEUS and EOB-MRI was 11 ± 13 days (Table 1).

Of the 133 lesions, 107 (80.5%) were detected on gray-scale US, 120 (90.2%) on CEUS, and 131 (98.5%) on EOB-MRI, showing that the detection rate was higher on EOB-MRI. The mean diameters were 22 ± 18 mm for 118 lesions detected by both CEUS and EOB-MRI, 6 mm for 2 lesions detected only by CEUS, and 6 ± 3 mm for 13 lesions detected only by EOB-MRI. The mean diameter of lesions detected only by EOB-MRI was significantly smaller than that for those detected by both CEUS and EOB-MRI ($p = 0.016$) (Table 2).

Of the 109 lesions diagnosed as liver metastases histopathologically or based on the follow-up, the AUCs for diagnosis were 0.906 for CEUS and 0.851 for EOB-MRI, with no significant difference ($p = 0.41$) (Figure 2). Based on a rating of 4 or 5 on the confidence scale on CEUS and EOB-MRI, 109 lesions were diagnosed as metastatic disease with sensitivity, specificity, PPV, NPV, and accuracy of 90.8%, 84.5%, 97.1%, 67.1%, and 90.2%, respectively, for CEUS, and 95.4%, 70.8%, 93.7%, 77.3%, and 91%, respectively, for EOB-MRI. The specificity and PPV of CEUS were higher than those of EOB-MRI, but the overall diagnostic accuracy was equivalent for both methods (Table 3).

DISCUSSION

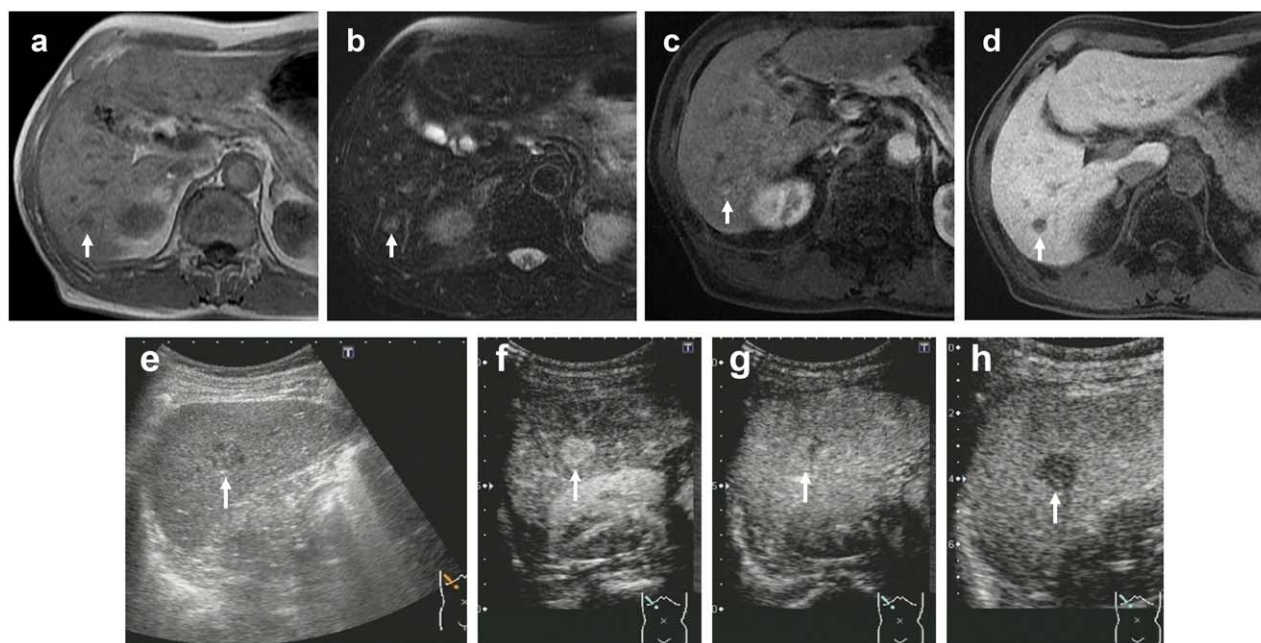Sonazoid is a contrast agent that consists of microbubbles of perfluorobutane gas stabilized

FIGURE 1. A 70-year-old man with a history of nonalcoholic steatohepatitis underwent surgical resection of transverse colon cancer. Follow-up imaging showed a 1.7-cm tumor in S6. **(A)** Gd-EOB-DTPA-enhanced MRI (EOB-MRI) shows a hypointense lesion in T1-weighted images (arrow). **(B)** EOB-MRI shows a hyperintense lesion in T2-weighted images (arrow). **(C)** EOB-MRI shows a hyperintense lesion in arterial phase (arrow). **(D)** EOB-MRI shows a hypointense lesion in hepatobiliary phase (arrow). The lesion had a diagnosis of liver metastasis (confidence scale 4). **(E)** Gray-scale US shows a hypoechoic lesion in S6 (arrow). **(F)** Contrast-enhanced US (CEUS) in arterial phase (40 seconds) shows hyperenhancing lesion (arrow). **(G)** CEUS shows isoenhancing lesion in late phase (arrow). The enhancement lasted more than 120 seconds. **(H)** CEUS shows hypoenhancing lesion in postvascular phase (arrow). The lesion had a diagnosis of not liver metastasis (confidence scale 1) from diagnostic criteria of CEUS, which was diagnosed hepatocellular carcinoma histopathologically.

TABLE 2
Comparison of the Detected Number of Hepatic Lesions on CEUS and EOB-MRI and the Tumor Diameter

	All Liver Tumors	CEUS and EOB-MRI	CEUS	EOB-MRI
Tumor numbers	133	118	2	13
Tumor size (mm) (mean $\pm$ SD)	21.3 $\pm$ 17.9	22.4 $\pm$ 18.0	5.5	6.3 $\pm$ 2.6*

Abbreviations: CEUS, contrast-enhanced ultrasonography; EOB-MRI: Gd-EOB-DTPA enhanced-MRI.
*CEUS and EOB-MRI versus EOB-MRI, $p = 0.016$.
$p < 0.05$; statistically significant.

by phospholipid monolayer shells with a median volume diameter of 2–3 μm. It is stable and resistant to sonographic exposure and radiates harmonic signals due to its low MI (0.2–0.3) at sufficient transmission power to allow continuous real-time imaging. Sonazoid is also taken up by Kupffer cells,[14,15] which have reduced function in malignant liver tumors such as HCC and liver metastases.[16–18] Therefore, the presence of a hypoechoic area (defect) in the liver parenchyma in the postvascular phase 10 minutes after Sonazoid injection is useful for diagnosis of malignant liver tumors such as HCC and metastases. For a tumor that was not visualized on initial gray-scale US but is observed as a defect in the postvascular phase, the dynamics of the contrast imaging of the lesion can be observed by reinjecting Sonazoid, enabling qualitative diagnosis.[11]

On the other hand, EOB is a contrast medium for MRI, which combines Gd-DTPA with an ethoxybenzyl group. A dynamic study can be performed using EOB, similarly to that with gadolinium contrast medium. In addition, the uptake of EOB is achieved by functional hepatocytes, which have the cloned organic anion transporting polypeptides (OATP1B3).[19] Contrast enhancement of hepatocytes reaches a maximum about 20 minutes after administration, and hypovascular hepatocellular nodules and small malignant tumors that are undetectable in a dynamic study can be detected in this phase.[20–23]
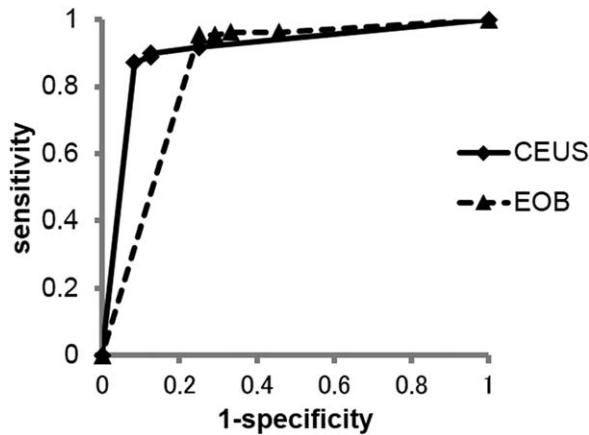
FIGURE 2. Receiver operating characteristic analysis curves for the diagnosis of liver metastasis of colorectal cancer using contrast-enhanced ultrasonography (CEUS) and Gd-EOB-DTPA enhanced-MRI (EOB-MRI).

TABLE 3
Sensitivity, Specificity, Positive-Predictive Value (PPV), Negative-Predictive Value (NPV), and Accuracy of CEUS and EOB-MRI Based on Confidence Scale of 4 or 5

Diagnostic Performance	CEUS	EOB-MRI
Sensitivity (%)	90.8	95.4
Specificity (%)	84.5	70.8
PPV (%)	97.1	93.7
NPV (%)	67.7	77.3
Accuracy (%)	90.2	91

Abbreviations: CEUS, contrast-enhanced ultrasonography; EOB-MRI, Gd-EOB-DTPA enhanced-MRI; NPV, negative predictive value; PPV, positive predictive value.

The recent development of CEUS with Sonazoid and EOB-MRI has improved the detection of malignant liver tumors such as HCC and metastatic disease.[24–26]

Hatanaka et al[7] have compared the diagnostic performance of CEUS with Sonazoid and contrast-enhanced CT in 113 patients with intrahepatic lesions that were likely to be malignant and found significantly higher sensitivity and diagnostic accuracy of CEUS. Because lesions are observed by low MI transmission power on CEUS with Sonazoid, as described above, hemodynamics can be repeatedly observed in real time. Evaluation in the vascular phase may be insufficient, but echo image dynamics can be re-evaluated using defect reperfusion imaging[11] by repeated intravenous injection of Sonazoid, which may explain the higher diagnostic sensitivity and accuracy. Hammerstingl et al[26] found that EOB-MRI was superior to contrast-enhanced CT for detection, diagnosis, and evaluation of treatment of liver tumors. Thus, both CEUS and EOB-MRI have been found to be superior to contrast-enhanced CT,[7,26] but to our knowledge, there has been no prospective comparison of CEUS and EOB-MRI in patients with liver metastasis of colorectal cancer.

There was no significant difference in AUC between CEUS and EOB-MRI, but the tumor detection rate and sensitivity were higher with EOB-MRI and the mean diameter of tumors detected by EOB-MRI alone was significantly smaller than that of tumors visualized by both CEUS and EOB-MRI. Huppertz et al[25] have compared the performance of EOB-MRI in the preoperative detection of lesions with the findings of intraoperative US and histopathological analysis in 131 patients with malignant liver tumors, including metastatic disease, and found that detection was improved by performing EOB-MRI before surgery, particularly for lesions of 10 mm or smaller. On CEUS, there are regions that are likely to become blind spots, such as the lateral segment of the left hepatic lobe near the stomach and segment S8 near the diaphragm. CEUS is also influenced by patient factors, such as obesity and inability to hold breath, as well as operator-dependent factors. In contrast, the whole liver can be objectively observed on EOB-MRI, which may account for the higher detection rate and sensitivity compared with CEUS. Muhi et al[10] have compared the diagnostic accuracy of contrast-enhanced CT, CEUS with Sonazoid, super paramagnetic iron oxide–MRI, and EOB-MRI in the evaluation of colorectal liver metastases retrospectively. They evaluated 113 patients with 112 colorectal liver metastases and found EOB-MRI was more accurate than CEUS for the evaluation of colorectal liver metastases.

In our prospective study, the specificity and PPV of CEUS were higher than those of EOB-MRI. CEUS has a superior temporal resolution and also permits repeated intravenous Sonazoid injection when lesions not visualized by gray-scale US are observed as defects in the postvascular phase. This allows reliable diagnosis by re-evaluation of the hemodynamics. Moreover, hemodynamics of the tumor cannot be evaluated in real time on EOB-MRI, unlike on CEUS. Thus, it may be difficult to make a definite diagnosis when the tumor is small. The higher specificity and PPV of CEUS may have been due to these factors. The NPV for diagnosis of liver metastasis by EOB-MRI was 77.3% in our study, which is lower than those in other reports.[27,28] Of the 133 lesions analyzed, 24 were diagnosed as tumors other than liver

metastasis, including 11 hepatic hemangiomas. The mean tumor diameter of these 11 lesions was 13 mm, which suggests that the low NPV was due to the difficulty of diagnosis of small-diameter hemangiomas on EOB-MRI in contrast with the use of defect reperfusion imaging in the postvascular phase with CEUS.

As limitations, first, this study includes the small sample size. Second, the final diagnosis of metastatic disease was also made based on imaging follow-up.

CONCLUSION

This study showed that EOB-MRI is useful for the detection of liver metastases of colorectal cancer, whereas CEUS with Sonazoid is useful for specific diagnosis of tumors thanks to real-time hemodynamics evaluation and defect reperfusion imaging. A combination of these two methods may improve detection and diagnosis of liver metastatic lesions of colorectal cancer.

REFERENCES

1. Yoon SS, Tanabe KK. Surgical treatment and other regional treatments for colorectal cancer liver metastases. Oncologist 1999;4:197.
2. Shimada H, Tanaka K, Endou I, et al. Treatment for colorectal liver metastases: a review. Langenbecks Arch Surg 2009;394:973.
3. Cavallari A, Vivarelli M, Bellusci R, et al. Liver metastases from colorectal cancer: present surgical approach. Hepatogastroenterology 2003;50:2067.
4. Mayo SC, Pawlik TM. Current management of colorectal hepatic metastasis. Expert Rev Gastroenterol Hepatol 2009;3:131.
5. Ryu SW, Bok GH, Jang JY, et al. Clinically useful diagnostic tool of contrast enhanced ultrasonography for focal liver masses: comparison to computed tomography and magnetic resonance imaging. Gut Liver 2014;8:292.
6. Mishima M, Toh U, Iwakuma N, et al. Evaluation of contrast Sonazoid-enhanced ultrasonography for the detection of hepatic metastases in breast cancer. Breast Cancer 2014;23:231.
7. Hatanaka K, Kudo M, Minami Y, et al. Sonazoid-enhanced ultrasonography for diagnosis of hepatic malignancies: comparison with contrast-enhanced CT. Oncology 2008;75:42.
8. Seneterre E, Taouel P, Bouvier Y, et al. Detection of hepatic metastases: ferumoxides enhanced MR imaging versus unenhanced MR imaging and CT during arterial portgraphy. Radiology 1996;200:785.
9. Nomura K, Kadoya M, Ueda K, et al. Detection of hepatic metastases from colorectal carcinoma: comparison of histopathologic features of anatomic resected liver with results of preoperative imaging. J Clin Gastroenterol 2007;41:789.
10. Muhi A, Ichikawa T, Motosugi U, et al. Diagnosis of colorectal hepatic metastases: comparison of contrast-enhanced CT, contrast-enhanced US, superparamagnetic iron oxide-enhanced MRI, and gadoxetic acid-enhanced MRI. J Magn Reson Imaging 2011;34:326.
11. Kudo M, Hatanaka K, Maekawa K. Newly developed novel sonographic technique, defect reperfusion sonographic imaging, using sonazoid in the management of hepatocellular carcinoma. Oncology 2010;78:40.
12. Claudon M, Dietrich CF, Choi BI, et al. Guidelines and good clinical practice recommendations for contrast enhanced sonographic (CEUS) in the liver—update 2012: a WFUMB-EFSUMB initiative in cooperation with representatives of AFSUMB, AIUM, ASUM, FLAUS and ICUS. Ultraschall Med 2013;34:11.
13. Zech CJ, Herrmann KA, Reiser MF, et al. MR imaging in patients with suspected liver metastases: value of liver-specific contrast agent Gd-EOB-DTPA. Magn Reson Med Sci 2007;6:43.
14. Yanagisawa K, Moriyasu F, Miyahara T, et al. Phagocytosis of ultrasound contrast agent microbubbles by Kupffer cells. Ultrasound Med Biol 2007;33:318.
15. Watanabe R, Matsumura M, Munemasa T, et al. Mechanism of hepatic parenchyma-specific contrast of microbubble-based contrast agent for ultrasonography: microscopic studies in rat liver. Invest Radiol 2007;42:643.
16. Sontum PC. Physicochemical characteristics of Sonazoid a new contrast agent for sonographic imaging. Ultrasound Med Biol 2008;34:824.
17. Watanabe R, Matsumura M, Chen CJ, et al. Characterization of tumor imaging with microbubble-based sonographic contrast agent, Sonazoid, in rabbit liver. Biol Pharm Bull 2005;28:972.
18. Hatanaka K, Kudo M, Minami Y, et al. Differential diagnosis of hepatic tumors: value of contrast-enhanced harmonic sonography using the newly developed contrast agent, Sonazoid. Intervirology 2008;51:61.
19. Ueno A, Masugi Y, Yamazaki K, et al. OATP1B3 expression is strongly associated with Wnt/β-catenin signaling and represents the transporter of gadoxetic acid in hepatocellular carcinoma. J Hepatol 2014;61:1080.
20. Vogl TJ, Kummel S, Hammerstingl R, et al. Liver tumors: comparison of MR imaging with Gd-EOB-DTPA and Gd-DTPA. Radiology 1996;201:59.
21. Reimer P, Rummeny E, Shamsi K, et al. Phase II clinical evaluation of Gd-EOB-DTPA: dose, safety aspects and pulse sequence. Radiology 1996;199:177.

22. Weinmann HJ, Schuhmann-Giampieri G, Schmitt-Willich H, et al. A new lipophilic gadolinium chelate as a tissue-specific contrast medium for MRI. Magn Reson Med 1991;22:233.

23. Schuhmann-Giampieri G, Schmitt-Willich H, Press WR, et al. Preclinical evaluation of Gd-EOB-DTPA as a contrast agent in MR imaging of the hepatobiliary system. Radiology 1992;183:59.

24. Kudo M, Hatanaka K, Kumada T, et al. Double-contrast sonographic: a novel surveillance tool for hepatocellular carcinoma. Am J Gastroenterol 2011;106:368.

25. Huppertz A, Balzer T, Blakeborough A, et al. Improved detection of focal liver lesions at MRI imaging: multicenter comparison of gadoxetic acid-enhanced MR images with intraoperative findings. Radiology 2004;230:266.

26. Hammerstingl R, Huppertz A, Breuer J, et al. Diagnostic efficacy of gadoxetic acid (Primovist)-enhanced MRI and spiral-CT for a therapeutic strategy: comparison with intraoperative and histopathologic findings in focal liver lesions. Eur Radiol 2008;18:457.

27. Wagnetz U, Atri M, Massey C, et al. Intraoperative sonographic of the liver in primary and secondary hepatic malignancies: comparison with preoperative 1.5-T MRI and 64-MDCT. AJR Am J Roentgenol 2011;196:562.

28. Seo HJ, Kim MJ, Lee JD, et al. Gadoxetate disodium-enhanced magnetic resonance imaging versus contrast-enhanced ^{18}F-fluorodeoxyglucose positron emission tomography/computed tomography for the detection of colorectal liver metastases. Invest Radiol 2011;46:548.